

Stress Analysis of Cylindrical Rock Discs Subjected to Axial Double Point Load

SYD S. PENG*

An axisymmetric finite element method was used to determine the stress distribution developed in cylindrical rock discs of various diameter/thickness ratios subjected to double point loading. The characteristics of tensile radial and tangential stress distributions were discussed in detail. Stress fields tend to stabilize when the ratio of diameter to thickness is larger than one. Due to the complexity of the stress field, it is rather difficult to develop a simplified tensile fracture strength criterion. But it is a reliable method of determining preferred orientation of fracture plane due to the predominance of tensile tangential stress.

INTRODUCTION

The double point loading test is being used to determine the apparent tensile strength [1, 2] and the anisotropic fracture characteristics of rocks and coal [3].

In the double point load test, a pair of hemispherical indentors of extremely small diameter are applied on the opposite sides of the central axis of a rock disc (Fig. 1). The advantage of this testing method is that the tolerance of specimen specification can be much more relaxed than those for uniaxial compressive and tensile strength tests. However, the stress field in the specimen due to double point loading has not been investigated thoroughly. The current practice of determining tensile strength by double point loading method is to use the formula developed by Frocht [4] for infinite elastic media; when a disc specimen is subjected to a vertical force, P , a tensile horizontal force of magnitude P/π , symmetrical with respect to the vertical section passing through the central axis, is developed in the specimen. The tensile strength of the specimen is then determined as:

$$\sigma_t = P/\pi DT \quad (1)$$

where σ_t = tensile strength, P = applied vertical force, D = diameter of the disc specimen, and T = thickness of the disc specimen.

This formula for determining the tensile strength of rocks is, of course, approximate and as mentioned earlier, its validity is not yet explored. For this purpose, the axisymmetric finite element method was used to analyze the stress field developed in specimens subjected to double point loading. The main concern was to determine the stress field induced by the double

point loading and how this stress field varies with specimen geometry.

THE FINITE ELEMENT MODEL

Figure 1 shows the cross-section (upper one) and jig (lower one) for the double point loading test. The applied load, $P = 16$ lb is an arbitrary chosen number. Due to its symmetry, only a quarter of this section is needed for finite element analysis. In the analysis, the thickness, t , is fixed at 2 in., but the radius, r , varies at 0.5, 1.0, 2.0 and 3 in., i.e. stress fields are determined for specimens with $r/t = 1/4, 1/2, 1$ and 1.5.

The finite element mesh layouts for each specimen geometry are shown in Figs. 2-5. The elements are isoparametric solid elements or eight-noded hexahedrons. The numbers of elements vary with specimen geometry as shown. However, the material properties are fixed with Young's modulus = 2×10^6 psi, and Poisson's ratio = 0.25.

RESULTS

From the axisymmetric finite element analysis, the stress distributions of four types of stress were obtained, i.e. axial, tangential, radial and shear stresses. Since the final specimen fracture under double point load were exclusively splitting along diametral plane [2, 3], they were tensile fracture and caused by tensile stresses. Therefore, in analyzing the stress distribution of specimens (subjected to double point loading) only these stresses that were in tensile mode needed to be considered. Consequently, only the tangential and radial stress distribution are presented and discussed in the following section (Figs. 2, 3 and 6-9).

* College of Mineral and Energy Resources, West Virginia University, Morgantown, WV 26506, U.S.A.

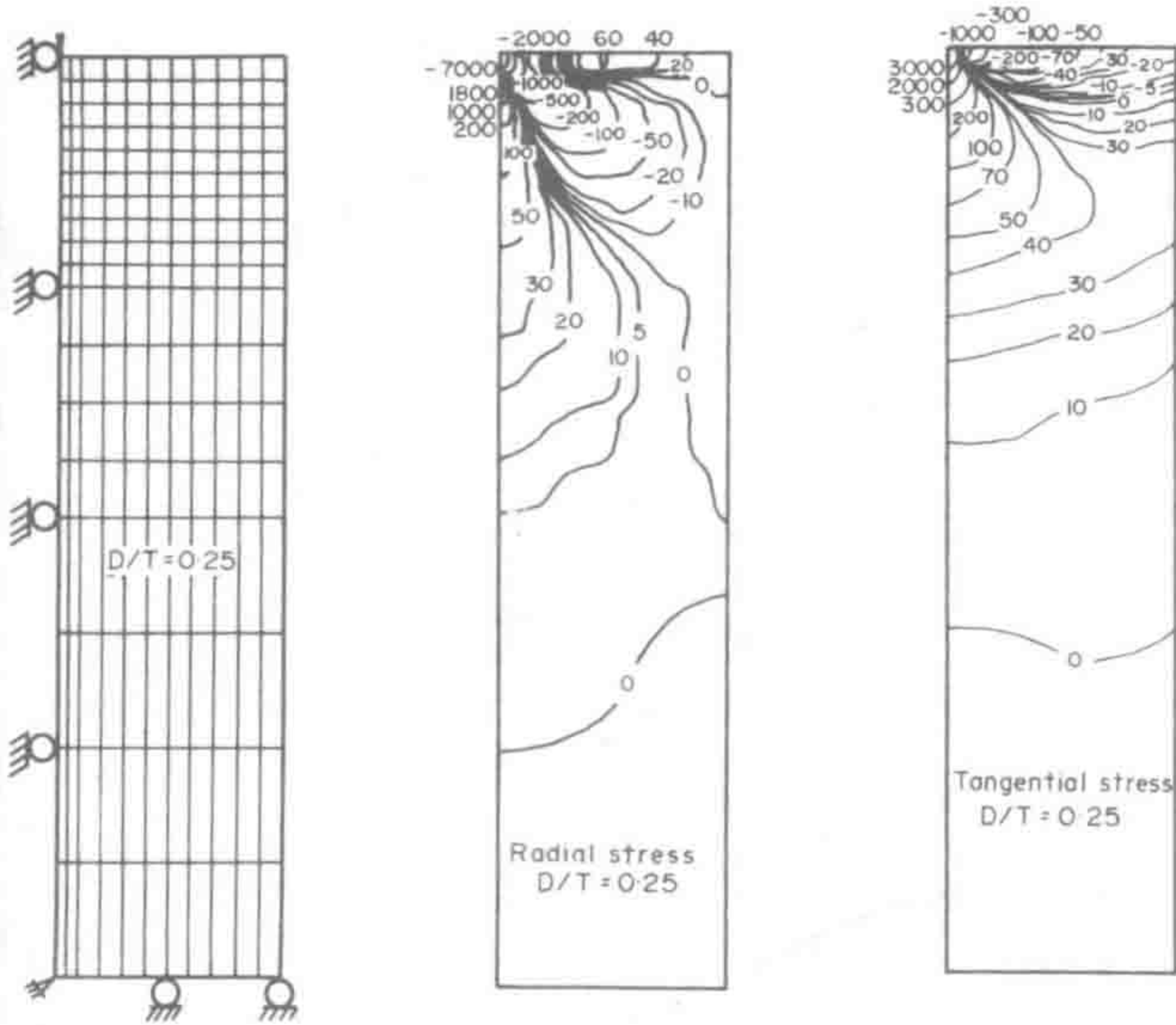


Fig. 2. Finite element mesh layouts and stress distributions for specimens with $D/T = 0.25$.

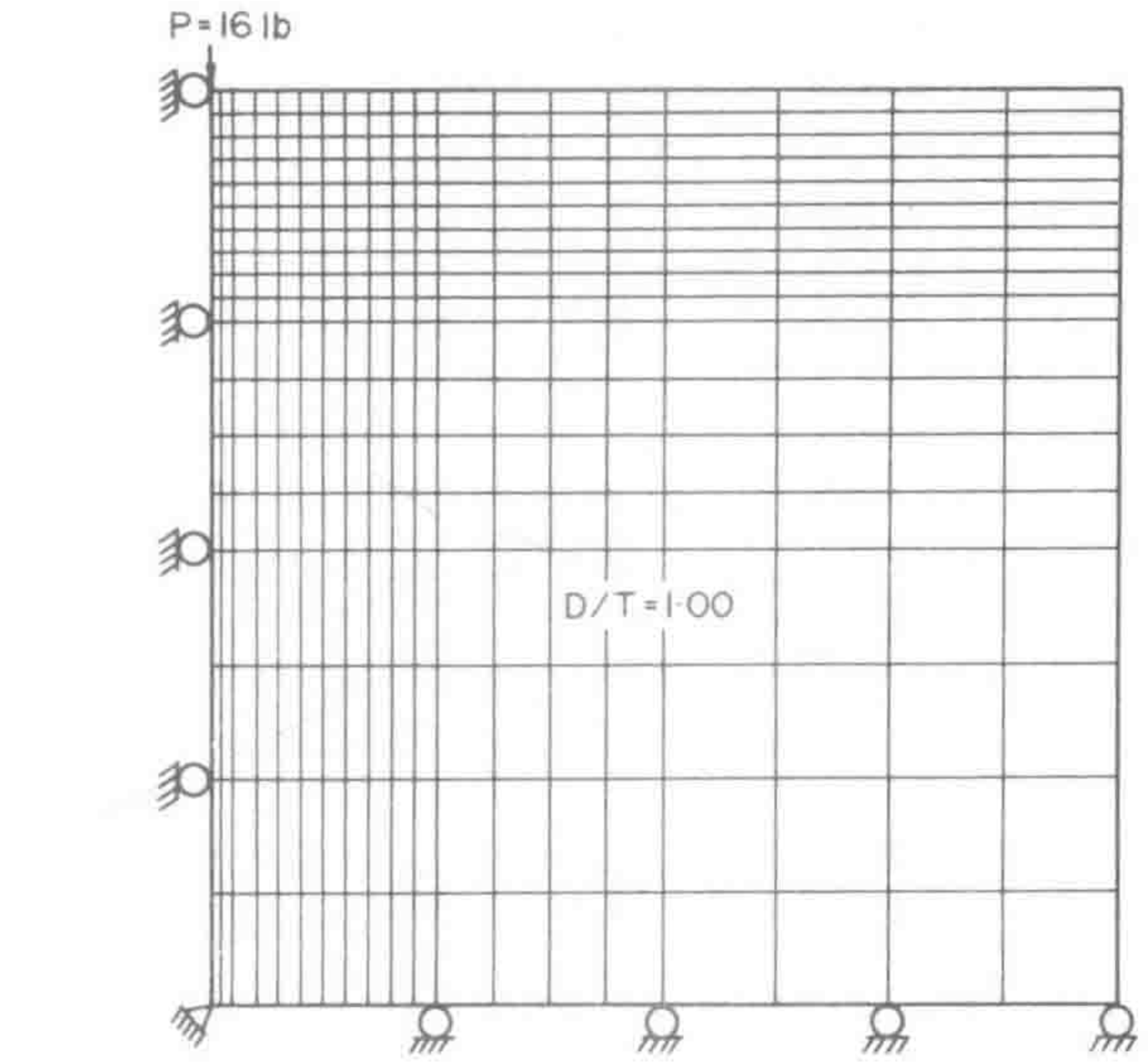


Fig. 4. Finite element mesh layouts for specimens with $D/T = 1.0$.

With the exception of the element where the load is applied, the tangential stress at the surface of the disc specimen is compressive. The highest occurs at the element immediately next to the right of the element where load is applied with 1122 psi. It decreases rapidly as it goes toward the circumference and the interior of the specimen. The maximum depth of this zone of compressive tangential stress is $T/38$ for $D/T = 0.25$. It increases and stabilizes at depth of $T/9$ for $D/T > 1.0$. The maximum tensile tangential stress increases slightly from 1122 psi for $D/T = 0.25$ to 1155 psi for $D/T > 1.0$.

It appears that the stress distribution for specimen with $D/T > 1.0$ is rather consistent and the effect of specimen geometry is insignificant when $D/T > 1.0$.

B. Radial stress distribution

Compressive radial stress occurs at the specimen surface with a radius of 0.15 in. (or $0.3r$ for $r = 0.5$ in.)

from the point where load is applied. The zone of compressive stress resembles the tail end of a trumpet with its axis fixed at approximately 40° from the specimen surface and its apex at the point where the load is applied. The maximum compressive radial stress is at the element where the load is applied with 7366 psi for $D/T = 0.25$. It decreases rapidly toward the tail end of the trumpet. The maximum compressive radial stress increases from 7366 psi for $D/T = 0.25$ to 7400 psi for $D/T > 0.75$.

Tensile radial stress occurs in all areas other than the trumpet-shaped zone mentioned earlier. The highest occurs at the element along the vertical axis and immediately below the element where the load is applied. It decreases rapidly while increases in area of tensile zone laterally as it goes down deeper toward the interior of the specimen. The maximum tensile radial stress is 1818 psi for $D/T = 0.25$ and decreases to 1800 psi for $D/T > 0.75$.

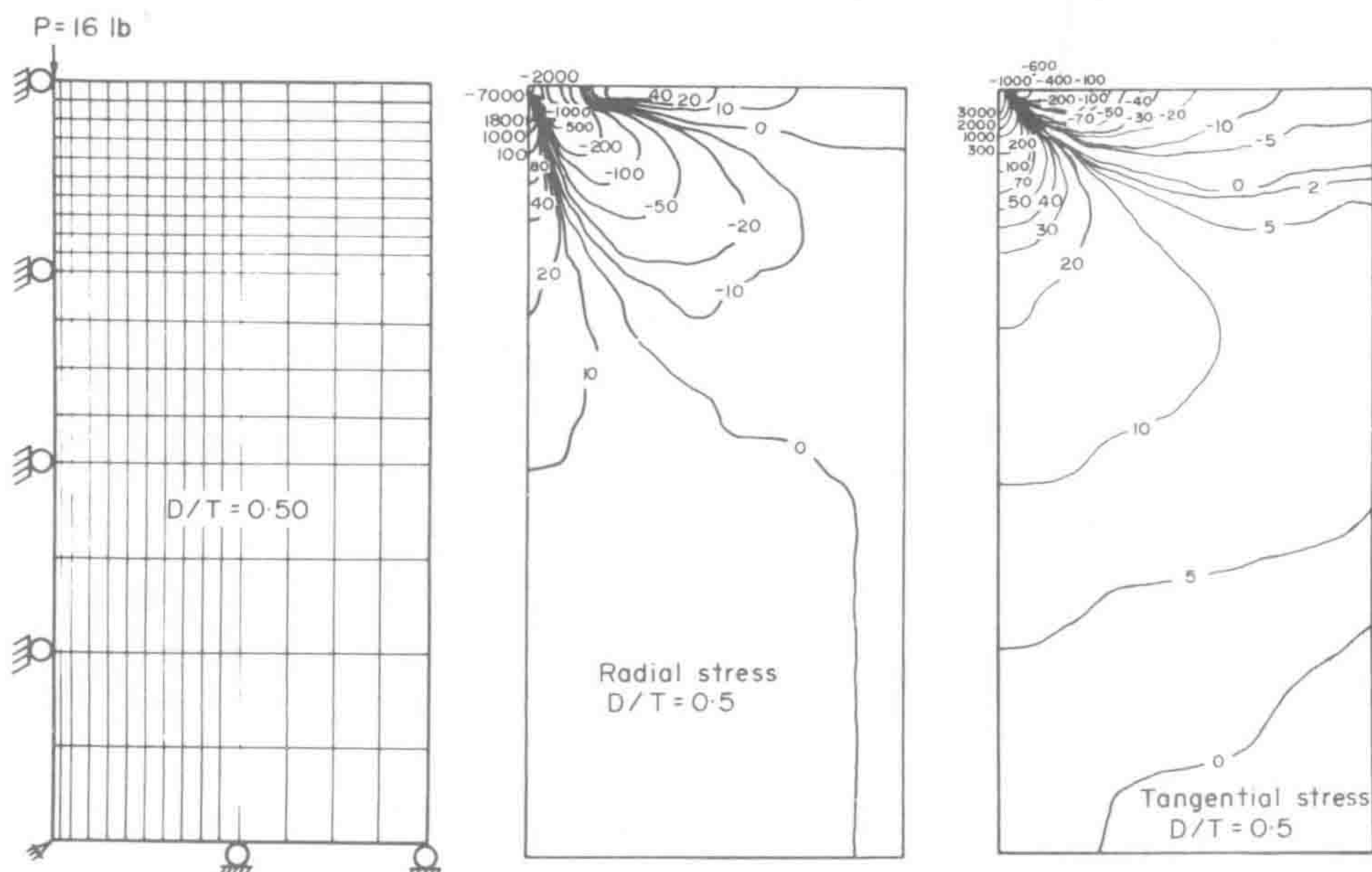


Fig. 3. Finite element mesh layouts and stress distributions for specimens with $D/T = 0.50$.

surface where compressive tangential stress prevails. Therefore, a biaxial tensile stress develops in the interior region where it shapes like an upside down bin hopper with the apex at the point of load application and the axis coinciding with the central axis of the specimen. With the exception of maximum tangential stress at the point of load application (where compressive radial stress develops), the magnitude of tensile radial stress is slightly lower than that of tensile tangential stress.

Since high tensile stresses develop beneath the point of load application and decreases rapidly away from the point of load application, fracture is expected to initiate at this area and propagate outward toward the edge and downward toward the center of the specimen. However, it must be cautioned that the area immediate to the point of load application tends to be crushed off due to the extremely high compressive axial stress and thus no high tensile radial and tangential stresses can be developed in the immediate vicinity of the point of load application. Therefore, the more exact phenomena leading to the specimen fracture are that cracks initiate at the vertical axis some depth below the point of load application due to biaxial (radial and tangential) tensile stresses. As soon as the crack forms, tensile tangential stress takes over and causes it to propagate radially. This radial crack may stop as it travels upward into the zone of compressive tangential stress if the kinetic energy of the moving crack is not large enough to overcome this obstacle. This is verified by the broken specimens tested by Sundae [2] that radial cracks propagate away from the center of the specimen and that some of these cracks do not reach the periphery or top or bottom surfaces of the specimens.

Equation (1) is based on the approximation that a point load of P will produce a tensile horizontal force of P/π which is about 5 lb in this research. An integration of the tangential stress obtained by finite element analysis indicates an average tensile force of 31.5 lb regardless of specimen geometry. In addition, the finite element analysis shows that the stress distribution changes slightly for specimens with $D/T < 0.75$

and stabilizes for specimens with $D/T > 1.00$. Therefore, tensile fracture strength should not vary considerably for specimens with $D/T > 1.00$. Thus, the best specimen geometry for double point load test is those with $D/T > 1.00$.

Due to the occurrence of tensile tangential stress in large portions of the specimen subjected to double point loading, the pre-existing cracks in the vertical plane play a significant role in specimen fracture. Crack tips serve as stress risers. Fractures propagate easier and faster if more cracks line up in the vertical plane. This could happen to large specimens and account for the lower tensile horizontal failure stress obtained [2].

The complexities of the stress distributions developed in a specimen subjected to double point load make it difficult to develop a theory to determine the stress at which complete specimen fracture occurs. It is, however, a reliable method of determining the preferred orientation of fracture plane due to the predominance of tensile tangential stress, and the fact that no restriction is imposed by the testing devices other than the two points where the load is applied. It is also a technique to define the limits over which a vertical fracture might grow in the hydraulic fracturing process. This information can be obtained by conducting tests on at least 1 ft intervals over the entire formation of interest. Such a breaking strength index log would be useful in selecting intervals to be perforated prior to the induced fracturing operation [5].

Received 4 June 1975.

REFERENCES

1. McWilliams J. R. The role of microstructure in the physical properties of rock, testing techniques for rock mechanics A.S.T.M. Spec. Tech. Pub. 402, pp. 175-189 (1966).
2. Sundae Laxman S. Effect of specimen volume on apparent tensile strength of three igneous rocks, U.S. Bur. Mines, Rept. Inv. 7846, 17 pp (1974).
3. Komar C. A., Overbey W. K., Jr and Pasini J., III. Directional properties of coal and their utilization in underground gasification experiments, U.S. Bur. Mines, TPR 73, 11 pp (1973).
4. Frocht M. M. *Photoelasticity* Vol. 2, p. 39, Wiley NY (1974).
5. Komar C. A. Personal communication.